

Extended Kalman Filtering for Flexible Joint Space Robot Control

Steve Ulrich, *Member, IEEE* and Jurek Z. Sasiadek, *Senior Member, IEEE*

Abstract—In this paper, an extended Kalman filter (EKF) strategy to estimate state variables from noisy measurements in flexible joint space manipulators is presented. First, an EKF that estimates the link and motor positions/velocities using only measurements from motor sensors is developed for space robots modeled with a classical linear joint dynamics model. Second, an extension for a novel nonlinear joint dynamics formulation is provided. The state estimates are coupled to a flexible joint adaptive controller in order to provide a complete closed-loop solution for real-time estimation and control. In numerical simulations, the EKF-adaptive controller combination demonstrates, for both dynamics representations, good performance when tracking a 12.6×12.6 m square trajectory.

I. INTRODUCTION

Ongoing worldwide space robotic activities concentrate on the development of lightweight and autonomous robotic manipulators designed specifically for on-orbit servicing operations [1]. For such space robot applications, the minimization of vibrations and accurate trajectory control with the minimum execution time are critical. However, the flexibility effects inherent to lightweight space robots equipped with harmonic drive gear mechanisms, such as the German Aerospace Center (DLR) Robotics Component Verification on the International Space Station (ROKVISS), make this objective a challenging task. In most cases, joint flexibility effect is the limiting factor to the achievable performance [2].

For such flexible manipulator systems, several controllers have been proposed in the literature. However, the vast majority of flexible joint control algorithms are classified as full-state feedback controllers. Full state feedback control requires the knowledge of four state variables: link and motor angular positions, \mathbf{q} and \mathbf{q}_m , and link and motor angular velocities, $\dot{\mathbf{q}}$ and $\dot{\mathbf{q}}_m$. Although some advanced space robot systems have access to measurements providing a knowledge of joint elasticity effects (for example, the DLR's Lightweight Robot III is equipped with joint torque sensors [3]), typical robot manipulators such as the Mitsubishi PA10-6CE are instrumented to measure only motor positions and velocities with an encoder and a tachometer on each motor axis of the manipulator [4].

Therefore, since the last few decades, several solutions to this state estimation problem have been proposed. The first

one consists in designing a nonlinear observer to compute one or more states in the flexible joint robot model. Nicosia *et al.* propose a procedure to construct approximate nonlinear observers in which an approach to derive observers based on the geometric nonlinear control theory is used in connection with an approximation technique [5]. Assuming as outputs the global link coordinates and their time derivatives, a nonlinear observer which reconstructs all state variables is proposed by Tomei [6]. Chatlatanagulchai *et al.* designed a neural network observer to determine link and motor positions/velocities and combine this observer with a robust controller [7]. Similarly, Abdollahi *et al.* present a stable neural network-based observer for flexible joint robots [8]. Nicosia and Tomei propose a controller for which only link positions are required to be available from measurements and where the other variables are provided by a nonlinear observer [9]. A global asymptotic link position tracking controller that only requires link and motor position measurements is proposed by Dixon *et al.* [10]. Specifically, in their work, the authors use a nonlinear link velocity filter in order to eliminate link velocity measurements while a set of linear filters is utilized to eliminate the need for motor velocity measurements. Kim and Lee designed an adaptive controller based on link and actuator position measurements only where link and motor velocity filters are used to estimate the unknown velocity terms [11]. A major problem with all these aforementioned methods is that link angular position measurements are required in the observation process.

Besides using a nonlinear observer, another solution to estimate in real-time state variables not available through measurements consists in applying the Kalman filter theory. Goudreau and Schwartz developed an extended Kalman filter (EKF) to estimate joint positions and velocities based on joint measurements and control torques for a direct-drive two-link rigid joint manipulator [12]. Lertpiriyasuwat and Burg proposed a Kalman Filter (KF) that combines end-effector position measurements obtained from a laser tracker sensor with joint angular position measurements to estimate end-effector and orientation in an industrial robot [13]. However, in these two studies the KF/EKF are designed based on a rigid joint dynamic representation.

Timcenko and Kircanski developed a linear Kalman filter to estimate the control torque in a flexible joint robot and used it in a feedforward/feedback controller scheme [14]. Hollars and Cannon used a constant-gain EKF (CGEKF) to estimate, for use by a state feedback control law, the state of a planar two-link robot arm with rigid links and flexibility in

The authors are with the Department of Mechanical and Aerospace Engineering, Carleton University, Ottawa, Ontario, K1S 5B6, Canada (phone: 613-520-2600 ext. 1833; e-mail: sulrich@connect.carleton.ca). Financial assistance from the Natural Sciences and Engineering Research Council of Canada (NSERC) is gratefully acknowledged.

its joints [15]. A significant advantage of the CGEKF approach is that the computational load is much less than that of the EKF. However, as stated in [16], the stability of such system must be carefully evaluated since the problem is inherently nonlinear. Recently, in 2010, Lightcap and Banks presented an Extended Kalman Filter (EKF) to estimate link and motor positions/velocities based on motor measurements [17]. Although their approach does not use directly link position measurements, a real-time knowledge of link positions is provided by sets of retro-reflective markers positioned on the links, which represent an uncommon sensor for robotic manipulators, especially for those operating in space. One major problem with these Kalman filter-based methodologies for flexible joint robots is that despite the fact that experimental studies have shown that flexible gears are much more complex than that of a linear spring [18], their design and simulation validation are based on the classical dynamic representation proposed by Spong [19] which models each joint as a linear torsional spring of constant stiffness.

The first contribution of this paper consists in the design of two EKFs that estimate link and motor positions/velocities for a flexible joint space robotic manipulator: (1) a first EKF is designed for a robot modeled with the classical Spong's linear joint model and (2) a second EKF is proposed for a space manipulator modeled with a novel nonlinear joint dynamics formulation recently proposed by Ulrich and Sasiadek [20]. While the second EKF expands upon previous work by incorporating nonlinear flexible effects such as nonlinear joint stiffness and soft-windup in the process model, both EKFs are novel in the sense that their applicability to a robot equipped only with motor encoders and tachometers is demonstrated. The second contribution of this study is the numerical evaluation of the resulting EKF-adaptive controller combinations for accurate closed-loop estimation and control of a flexible joint space robot.

II. DYNAMICS MODELING

A. Linear Joint Model

The classical dynamics equation of a multilink robot with rigid links and flexible joints proposed by Spong [19] is derived in terms of kinetic and potential energies stored in the system by the Euler-Lagrange formulation. With this model, each joint is modeled as a linear torsional spring of constant stiffness and the resulting dynamics of flexible joint manipulators consists in two second-order differential equations. Omitting the gravity term for space robot applications, the resulting linear joint dynamics model is given by

$$\mathbf{M}(\mathbf{q})\ddot{\mathbf{q}} + \mathbf{C}(\mathbf{q}, \dot{\mathbf{q}})\dot{\mathbf{q}} - \mathbf{k}(\mathbf{q}_m - \mathbf{q}) = \mathbf{0} \quad (1)$$

$$\mathbf{J}_m \ddot{\mathbf{q}}_m + \mathbf{k}(\mathbf{q}_m - \mathbf{q}) = \boldsymbol{\tau}, \quad (2)$$

Where \mathbf{q} is the link angle vector, \mathbf{q}_m is the vector denoting

the angular displacements of the motor shaft angles, $\mathbf{M}(\mathbf{q})$ is the symmetric and positive definite rigid inertia matrix, $\boldsymbol{\tau}$ is the control torque vector, $\mathbf{C}(\mathbf{q}, \dot{\mathbf{q}})$ is a matrix comprising Coriolis and centrifugal effects, \mathbf{k} is the diagonal and positive definite stiffness matrix of the joints and where \mathbf{J}_m denotes the positive definite motor inertia matrix. For a two-link robot, $\mathbf{M}(\mathbf{q})$ and $\mathbf{C}(\mathbf{q}, \dot{\mathbf{q}})$ are given by [19]

$$\mathbf{M}(\mathbf{q}) = \begin{bmatrix} M_{11} & M_{12} \\ M_{21} & M_{22} \end{bmatrix}, \quad (3)$$

with

$$M_{11} = m_1 l_{c1}^2 + m_2 (l_1^2 + l_{c2}^2 + 2l_1 l_{c2} \cos q_2) + I_1 + I_2 \quad (4)$$

$$M_{12} = M_{21} = m_2 (l_{c2}^2 + l_1 l_{c2} \cos q_2) + I_2 \quad (5)$$

$$M_{22} = m_2 l_{c2}^2 + I_2 \quad (6)$$

and $\mathbf{C}(\mathbf{q}, \dot{\mathbf{q}})$ is given by

$$\mathbf{C}(\mathbf{q}, \dot{\mathbf{q}}) = -m_2 l_1 l_{c2} \sin q_2 \begin{bmatrix} \dot{q}_2 & \dot{q}_1 + \dot{q}_2 \\ -\dot{q}_1 & 0 \end{bmatrix}, \quad (7)$$

where, for $i = 1, 2$, m_i denotes the mass of link i , I_i represents the inertia of link i , l_i denotes the length of link i and l_{ci} denotes the distance from the previous joint to center of gravity of link i . Equations (1) and (2) can be solved for the link and motor acceleration, as follows

$$\ddot{\mathbf{q}} = \mathbf{M}^{-1}(\mathbf{q})[\mathbf{k}(\mathbf{q}_m - \mathbf{q}) - \mathbf{C}(\mathbf{q}, \dot{\mathbf{q}})\dot{\mathbf{q}}] \quad (8)$$

$$\ddot{\mathbf{q}}_m = \mathbf{J}_m^{-1}[\boldsymbol{\tau} - \mathbf{k}(\mathbf{q}_m - \mathbf{q})]. \quad (9)$$

B. Nonlinear Joint Model

Although the linear joint model is considered as the centerpiece of nearly all work in the area of flexible joint control, experimental studies have shown that flexible gears are much more complex than that of a linear spring [18, 21]. By combining the effects of the nonlinear stiffness torque term, soft-windup, frictional losses, and inertial cross-coupling, the following nonlinear joint dynamics model was recently proposed by Ulrich and Sasiadek [20]

$$\mathbf{M}(\mathbf{q})\ddot{\mathbf{q}} + \mathbf{S}\ddot{\mathbf{q}}_m + \mathbf{C}(\mathbf{q}, \dot{\mathbf{q}})\dot{\mathbf{q}} + \mathbf{f}(\dot{\mathbf{q}}) - \mathbf{k}(\mathbf{q}, \mathbf{q}_m)(\mathbf{q}_m - \mathbf{q}) = \mathbf{0} \quad (10)$$

$$\mathbf{J}_m \ddot{\mathbf{q}}_m + \mathbf{S}^T \ddot{\mathbf{q}} + \mathbf{k}(\mathbf{q}, \mathbf{q}_m)(\mathbf{q}_m - \mathbf{q}) = \boldsymbol{\tau}, \quad (11)$$

where the matrix \mathbf{S} represents the inertial cross-coupling between motor and link accelerations and where the nonlinear stiffness matrix $\mathbf{k}(\mathbf{q}, \mathbf{q}_m)$ is given by

$$\mathbf{k}(\mathbf{q}, \mathbf{q}_m) = \mathbf{a}_1 \begin{bmatrix} (q_{m1} - q_1)^2 \\ (q_{m2} - q_2)^2 \end{bmatrix} + \mathbf{a}_2 + \mathbf{K}_{sw}(\mathbf{q}, \mathbf{q}_m) \quad (12)$$

where \mathbf{a}_1 and \mathbf{a}_2 are positive definite diagonal matrices of stiffness coefficients and $\mathbf{K}_{sw}(\mathbf{q}, \mathbf{q}_m)$ is the soft-windup correction factor that is modeled as a saddle-shaped function

$$\mathbf{K}_{sw}(\mathbf{q}, \mathbf{q}_m) = -\mathbf{k}_{sw} \begin{bmatrix} e^{-a_{sw}(q_{m1}-q_1)^2} & 0 \\ 0 & e^{-a_{sw}(q_{m2}-q_2)^2} \end{bmatrix}, \quad (13)$$

with \mathbf{k}_{sw} and a_{sw} being parameters defining the soft-windup function. In Eq. (10), $\mathbf{f}(\dot{\mathbf{q}})$ denotes the friction torque assumed to have the following nonlinear parametrizable form

$$\mathbf{f}(\dot{\mathbf{q}}) = \gamma_1 [\tanh(\gamma_2 \dot{\mathbf{q}}) - \tanh(\gamma_3 \dot{\mathbf{q}})] + \gamma_4 \tanh(\gamma_5 \dot{\mathbf{q}}) + \gamma_6 \dot{\mathbf{q}}, \quad (14)$$

where, for $i=1, \dots, 6$, γ_i denotes positive parameters defining the different friction components. As a result, the link and motor acceleration can be written as

$$\ddot{\mathbf{q}} = \mathbf{M}^{-1}(\mathbf{q}) [\mathbf{k}(\mathbf{q}, \mathbf{q}_m)(\mathbf{q}_m - \mathbf{q}) - \mathbf{f}(\dot{\mathbf{q}}) - \mathbf{C}(\mathbf{q}, \dot{\mathbf{q}})\dot{\mathbf{q}} - \mathbf{S}\ddot{\mathbf{q}}_m] \quad (15)$$

$$\ddot{\mathbf{q}}_m = \mathbf{J}_m^{-1} [\boldsymbol{\tau} - \mathbf{k}(\mathbf{q}, \mathbf{q}_m)(\mathbf{q}_m - \mathbf{q}) - \mathbf{S}^T \dot{\mathbf{q}}]. \quad (16)$$

III. DISCRETE-TIME EXTENDED KALMAN FILTER

For completeness, a brief review of the EKF theory [22], in its discrete form, is summarized in this section. Let a nonlinear system be described by the following dynamics equation

$$\mathbf{x}_{k+1} = f(\mathbf{x}_k, \mathbf{u}_k, \mathbf{w}_k) \quad (17)$$

and whose observations are described by the nonlinear measurement equation

$$\mathbf{z}_k = h(\mathbf{x}_k, \mathbf{v}_k), \quad (18)$$

where \mathbf{x}_k is the state vector, \mathbf{w}_k is the process noise, and \mathbf{z}_k and \mathbf{v}_k are the measurement vector and the measurement noise, respectively, at a discrete time t_k . It is assumed that \mathbf{w}_k and \mathbf{v}_k are uncorrelated, zero-mean Gaussian noises with covariances

$$E[\mathbf{w}_k \mathbf{w}_k^T] = \mathbf{Q}_k, \quad (19)$$

$$E[\mathbf{v}_k \mathbf{v}_k^T] = \mathbf{R}_k, \quad (20)$$

where $E[\]$ denotes the expectation. The initial mean and covariance of the state vector are given by

$$\hat{\mathbf{x}}_0 = E[\mathbf{x}_0], \quad (21)$$

$$\mathbf{P}_0 = E[(\mathbf{x}_0 - \hat{\mathbf{x}}_0)(\mathbf{x}_0 - \hat{\mathbf{x}}_0)^T]. \quad (22)$$

where \mathbf{x}_0 is uncorrelated with \mathbf{w}_k and \mathbf{v}_k .

Given the initial mean and the state covariance matrix and before taking into account any measurements, the state

estimate at time t is defined by

$$\hat{\mathbf{x}}_k = E[\mathbf{x}_k], \quad (23)$$

where $\hat{\ }^{\wedge}$ denotes the estimate. This predicted estimate satisfies the following differential equation

$$\dot{\hat{\mathbf{x}}}_{k+1} = E[f(\mathbf{x}_k, \mathbf{u}_k)] \equiv f(\hat{\mathbf{x}}_k, \mathbf{u}_k), \quad (24)$$

which may be integrated to give $\hat{\mathbf{x}}_{k+1}^-$, the *a priori*, or the propagated, state vector. Although the propagation of the state vector is performed with the nonlinear model of the dynamics, the propagation of state error covariance matrix, which is defined by

$$\mathbf{P}_k = E[(\mathbf{x}_k - \hat{\mathbf{x}}_k)(\mathbf{x}_k - \hat{\mathbf{x}}_k)^T], \quad (25)$$

is done with the discrete-time linear model of the system, as follows

$$\mathbf{P}_{k+1}^- = \mathbf{F}_k \mathbf{P}_k \mathbf{F}_k^T + \mathbf{Q}_k, \quad (26)$$

where \mathbf{P}_{k+1}^- is the *a priori*, or propagated, state error covariance matrix and where \mathbf{F}_k is the discrete state transition matrix given by

$$\mathbf{F}_k \equiv \boldsymbol{\Phi}_k = \left. \frac{\partial}{\partial \mathbf{x}_k} f(\mathbf{x}_k, t) \right|_{\hat{\mathbf{x}}_{k+1}^-}. \quad (27)$$

Following a measurement, the predicted state vector is updated in order to take into account the measurement

$$\hat{\mathbf{x}}_{k+1}^+ = \hat{\mathbf{x}}_{k+1}^- + \mathbf{K}_{k+1} (\mathbf{z}_k - \hat{\mathbf{z}}_k), \quad (28)$$

where $\hat{\mathbf{x}}_{k+1}^+$ is the *a posteriori*, or the estimated state vector, and where the predicted measurement $\hat{\mathbf{z}}_k$ is

$$\hat{\mathbf{z}}_k = h(\hat{\mathbf{x}}_{k+1}^-). \quad (29)$$

In Eq. (28), \mathbf{K}_{k+1} is the Kalman gain given by

$$\mathbf{K}_{k+1} = \mathbf{P}_{k+1}^- \mathbf{H}_k^T (\mathbf{H}_k \mathbf{P}_{k+1}^- \mathbf{H}_k^T + \mathbf{R}_k)^{-1}, \quad (30)$$

where

$$\mathbf{H}_k = \left. \frac{\partial}{\partial \mathbf{x}} h(\mathbf{x}) \right|_{\hat{\mathbf{x}}_{k+1}^-}. \quad (31)$$

Finally, the state error covariance matrix is updated by

$$\mathbf{P}_{k+1}^+ = \mathbf{P}_{k+1}^- - \mathbf{K}_{k+1} (\mathbf{H}_k \mathbf{P}_{k+1}^- \mathbf{H}_k^T + \mathbf{R}_k) \mathbf{K}_{k+1}^T. \quad (32)$$

In Eq. (28), the term $(\mathbf{z}_k - \hat{\mathbf{z}}_k)$ is called the residuals, or innovations. It reflects the degree to which the model fits the data.

IV. FLEXIBLE JOINT ROBOT ESTIMATION

In this section, the discrete-time EKF equations are applied to both the linear and nonlinear joint model.

A. Linear Joint Model Estimation

Let the state vector be defined by

$$\mathbf{x} = [\mathbf{q} \quad \dot{\mathbf{q}} \quad \mathbf{q}_m \quad \dot{\mathbf{q}}_m]^T \quad (33)$$

Such that the partial derivative of the robot dynamics with respect to the states can be written as

$$\frac{\partial \mathbf{f}}{\partial \mathbf{x}} = \mathbf{F} = \begin{bmatrix} \mathbf{0} & \mathbf{I}_2 & \mathbf{0} & \mathbf{0} \\ \mathbf{F}_{21} & \mathbf{F}_{22} & \mathbf{F}_{23} & \mathbf{0} \\ \mathbf{0} & \mathbf{0} & \mathbf{0} & \mathbf{I}_2 \\ \mathbf{F}_{41} & \mathbf{0} & \mathbf{F}_{43} & \mathbf{0} \end{bmatrix} \quad (34)$$

where

$$\mathbf{F}_{21} = -\mathbf{M}^{-1}(\mathbf{q}) \left[\frac{\partial \mathbf{M}(\mathbf{q})}{\partial \mathbf{q}} \ddot{\mathbf{q}} + \frac{\partial \mathbf{C}(\mathbf{q}, \dot{\mathbf{q}})}{\partial \mathbf{q}} \dot{\mathbf{q}} + \mathbf{k} \right] \quad (35)$$

$$\mathbf{F}_{22} = -\mathbf{M}^{-1}(\mathbf{q}) \left[\frac{\partial \mathbf{C}(\mathbf{q}, \dot{\mathbf{q}})}{\partial \dot{\mathbf{q}}} \dot{\mathbf{q}} + \mathbf{C}(\mathbf{q}, \dot{\mathbf{q}}) \right] \quad (36)$$

$$\mathbf{F}_{23} = \mathbf{M}^{-1}(\mathbf{q}) \mathbf{k} \quad (37)$$

$$\mathbf{F}_{41} = -\mathbf{F}_{43} = \mathbf{J}_m^{-1} \mathbf{k} \quad (38)$$

where expressions for link accelerations defined in Eq. (8) can be substituted in \mathbf{F}_{21} . In \mathbf{F}_{21} , the partial derivative of the robot inertia matrix and Coriolis matrix with respect to the link angle vector is given by

$$\frac{\partial \mathbf{M}(\mathbf{q})}{\partial \mathbf{q}} \ddot{\mathbf{q}} = -m_2 l_1 l_{c2} \sin q_2 \begin{bmatrix} 0 & 2\ddot{q}_1 + \ddot{q}_2 \\ 0 & \ddot{q}_1 \end{bmatrix} \quad (39)$$

$$\frac{\partial \mathbf{C}(\mathbf{q})}{\partial \mathbf{q}} \dot{\mathbf{q}} = -m_2 l_1 l_{c2} \cos q_2 \begin{bmatrix} 0 & \dot{q}_1 \dot{q}_2 + \dot{q}_2 (\dot{q}_1 + \dot{q}_2) \\ 0 & -\dot{q}_1^2 \end{bmatrix} \quad (40)$$

and the partial derivative necessary for \mathbf{F}_{22} is given by

$$\frac{\partial \mathbf{C}(\mathbf{q})}{\partial \dot{\mathbf{q}}} \dot{\mathbf{q}} = -m_2 l_1 l_{c2} \sin q_2 \begin{bmatrix} \dot{q}_2 & (\dot{q}_1 + \dot{q}_2) \\ -\dot{q}_1 & 0 \end{bmatrix} \quad (41)$$

Considering that the only measurements are provided by an encoder and tachometer on the motor sides, let define the measurement model as

$$h(\mathbf{x}) = [\mathbf{q}_m \quad \dot{\mathbf{q}}_m]^T \quad (42)$$

The linearization of this measurement model for the robot dynamics is as follows

$$\frac{\partial h}{\partial \mathbf{x}} = \mathbf{H} = \begin{bmatrix} \mathbf{0} & \mathbf{0} & \mathbf{I}_2 & \mathbf{0} \\ \mathbf{0} & \mathbf{0} & \mathbf{0} & \mathbf{I}_2 \end{bmatrix}^T \quad (43)$$

B. Nonlinear Joint Model Estimation

Considering the nonlinear joint model presented in Section II, the partial derivatives of the robot dynamics are

$$\mathbf{F}_{21} = -\mathbf{M}^{-1}(\mathbf{q}) \left[\frac{\partial \mathbf{M}(\mathbf{q})}{\partial \mathbf{q}} \ddot{\mathbf{q}} + \frac{\partial \mathbf{C}(\mathbf{q}, \dot{\mathbf{q}})}{\partial \mathbf{q}} \dot{\mathbf{q}} - \frac{\partial \mathbf{k}(\mathbf{q}, \mathbf{q}_m)}{\partial \mathbf{q}} (\mathbf{q}_m - \mathbf{q}) + \mathbf{k}(\mathbf{q}, \mathbf{q}_m) \right], \quad (44)$$

$$\mathbf{F}_{22} = -\mathbf{M}^{-1}(\mathbf{q}) \left[\frac{\partial \mathbf{C}(\mathbf{q}, \dot{\mathbf{q}})}{\partial \dot{\mathbf{q}}} \dot{\mathbf{q}} + \frac{\partial \mathbf{f}(\dot{\mathbf{q}})}{\partial \dot{\mathbf{q}}} + \mathbf{C}(\mathbf{q}, \dot{\mathbf{q}}) \right], \quad (45)$$

$$\mathbf{F}_{23} = \mathbf{M}^{-1}(\mathbf{q}) \left[\frac{\partial \mathbf{k}(\mathbf{q}, \mathbf{q}_m)}{\partial \mathbf{q}_m} (\mathbf{q}_m - \mathbf{q}) + \mathbf{k}(\mathbf{q}, \mathbf{q}_m) \right], \quad (46)$$

$$\mathbf{F}_{41} = -\mathbf{J}_m^{-1} \left[\frac{\partial \mathbf{k}(\mathbf{q}, \mathbf{q}_m)}{\partial \mathbf{q}} (\mathbf{q}_m - \mathbf{q}) - \mathbf{k}(\mathbf{q}, \mathbf{q}_m) \right], \quad (47)$$

$$\mathbf{F}_{43} = -\mathbf{J}_m^{-1} \left[\frac{\partial \mathbf{k}(\mathbf{q}, \mathbf{q}_m)}{\partial \mathbf{q}_m} (\mathbf{q}_m - \mathbf{q}) + \mathbf{k}(\mathbf{q}, \mathbf{q}_m) \right], \quad (48)$$

where

$$\frac{\partial \mathbf{k}(\mathbf{q}, \mathbf{q}_m)}{\partial \mathbf{q}} (\mathbf{q}_m - \mathbf{q}) = -\frac{\partial \mathbf{k}(\mathbf{q}, \mathbf{q}_m)}{\partial \mathbf{q}_m} (\mathbf{q}_m - \mathbf{q}) = \begin{bmatrix} a & 0 \\ 0 & b \end{bmatrix}, \quad (49)$$

$$\frac{\partial \mathbf{f}(\dot{\mathbf{q}})}{\partial \dot{\mathbf{q}}} = \begin{bmatrix} \frac{\partial \mathbf{f}(\dot{\mathbf{q}})}{\partial \dot{q}_1} & \frac{\partial \mathbf{f}(\dot{\mathbf{q}})}{\partial \dot{q}_2} \end{bmatrix} = \begin{bmatrix} c & 0 \\ 0 & d \end{bmatrix} \quad (50)$$

with

$$a = -2(q_{m1} - q_1)^2 [a_{111} + k_{sw11} a_{sw} e^{-a_{sw}(q_{m1} - q_1)^2}], \quad (51)$$

$$b = -2(q_{m2} - q_2)^2 [a_{122} + k_{sw22} a_{sw} e^{-a_{sw}(q_{m2} - q_2)^2}], \quad (52)$$

$$c = \gamma_1 [\gamma_2 \operatorname{sech}^2(\gamma_2 \dot{q}_1) - \gamma_3 \operatorname{sech}^2(\gamma_3 \dot{q}_1)] + \gamma_4 \gamma_5 \operatorname{sech}^2(\gamma_5 \dot{q}_1) + \gamma_6, \quad (53)$$

$$d = \gamma_1 [\gamma_2 \operatorname{sech}^2(\gamma_2 \dot{q}_2) - \gamma_3 \operatorname{sech}^2(\gamma_3 \dot{q}_2)] + \gamma_4 \gamma_5 \operatorname{sech}^2(\gamma_5 \dot{q}_2) + \gamma_6. \quad (54)$$

V. SIMULATION RESULTS

In this section, the linear joint-based EKF is applied to linear joint dynamics, and the nonlinear joint-based EKF is applied to nonlinear joint dynamics. To assess the performance of the estimators, a 12.6×12.6 m square trajectory was required to be tracked in 60 sec. with constant velocity by the endpoint of a two-link flexible joint space

robot for which the shoulder joint coincides with the fixed base of the robot located at the center of the square trajectory. For this application, the direct adaptive controller proposed in [23] is used. The parameters of the flexible joint robot are: $l_1=l_2=4.5$ m, $m_1=m_2=1.5075$ kg, $\mathbf{J}_m = \text{diag}[1]$ kg·m² and $\mathbf{k} = \text{diag}[500]$ N·m/rad. The parameters for the nonlinear joint dynamics model are chosen as $\mathbf{a}_1 = \mathbf{a}_2 = \text{diag}[500]$ N·m/rad, $\mathbf{k}_{sw} = \text{diag}[10]$ $a_{sw} = 3000$, $\mathbf{S} = \begin{bmatrix} 0 & J_{m2} \\ 0 & 0 \end{bmatrix}$, $\gamma_1 = 0.5$, $\gamma_2 = 150$, $\gamma_3 = 50$, $\gamma_4 = 2$, $\gamma_5 = 100$, and $\gamma_6 = 0.5$. The adaptive controller parameters are selected as $\Gamma_{pp} = \Gamma_{pi} = 150$, $\Gamma_{dp} = \Gamma_{di} = 25$, $\mathbf{K}_v = \text{diag}[35]$, and $\delta_p = 0.008$ and $\delta_d = 0.023$. Random zero-mean Gaussian noise with standard deviation of 1 deg and 1 deg/s were added to the measurement of each motor angular position and velocity, respectively. The sampling frequency for both sensors is 100 kHz.

Figures 1 and 2 illustrate the state estimation errors for both estimators. From these results, it can be seen that both EKFs provide good estimation accuracy since the estimation errors remain small in spite of large measurement noises. Figures 3 and 4 show the results of tracking endpoint trajectories with both EKF-adaptive controller combinations in a counter-clockwise direction starting at the lower-right-hand corner. As shown in Fig. 3, the linear joint-based strategy exhibits minimal overshoots at each corner of the trajectory. On the other hand, the nonlinear joint-based strategy yields slightly degraded performance, as shown in Fig. 4. Despite the fact that both EKFs yield a similar estimation accuracy, this slight decrease in trajectory tracking performance for the nonlinear joint dynamics is due to the addition of the highly nonlinear effects and friction torques which makes the control task more difficult. Finally, it must be noted that when the linear joint-based EKF is applied to the nonlinear joint dynamic model, the estimation results diverge, resulting in an unstable trajectory. This illustrates the benefits of using the nonlinear joint-based EKF in an actual application, where the dynamics of the manipulator is likely to be affected by highly nonlinear effects, such as inertial cross-coupling and friction.

VI. CONCLUSION

In this paper, an extended Kalman filter (EKF) estimator using only motor encoders and tachometers has been developed for a flexible joint space robot modeled with both the well-established Spong's linear joint dynamics model and a novel nonlinear joint dynamics model. Both EKFs were combined to a direct adaptive controller for which the controller gains are adapted in real-time. The resulting novel estimation and control systems were evaluated in closed-loop numerical simulations which demonstrated that good estimation and tracking performance are achieved while tracking a square trajectory by a flexible joint space robot.

REFERENCES

- [1] D. Reintsema, K. Landzettel and G. Hirzinger, "DLRs advanced telerobotic concepts and experiments for on-orbit servicing," In *Classics in Applied Mathematics Series*, Springer, 2007.
- [2] M. W. Spong, S. Hutchinson and M. Vidyasagar, *Robot Modeling and Control*. Hoboken, NJ: John Wiley and Sons Inc., 2006, pp. 220-221.
- [3] N. Sporer, DLR Light Weight Robot III Data Sheet, German Aerospace Center Institute of Robotics and Mechatronics.
- [4] C. A. Lightcap, "Measurement and control issues in a novel dynamic radiographic imaging system," Ph.D. thesis, University of Florida, 2008.
- [5] S. Nicosia, P. Tomei, and A. Tornambe, "A nonlinear observer for elastic robots," *IEEE J. Robot. Autom.*, vol. 4, no. 1, pp. 45-52, Feb. 1988.
- [6] P. Tomei, "An observer for flexible joint robots," *IEEE Trans. Autom. Control*, vol. 35, no. 6, pp. 739-743, Jun. 1990.
- [7] W. Chatlatanagulchai, H. C. Nho, and P. Meckl, "Robust observer backstepping neural network control of flexible-joint manipulators," in *Proc. Amer. Control Conf.*, Boston, MA, Jun. 2004, pp. 1154-1159.
- [8] F. Abdollahi, H. A. Talebi and R. V. Patel, "A stable neural network-based observer with application to flexible-joint manipulators," *IEEE Trans. Neural Net.*, vol. 17, no. 1, pp. 118-129, 2006.
- [9] S. Nicosia and P. Tomei, "A tracking controller for flexible-joint robots using only link position feedback," *IEEE Trans. Autom. Control*, vol. 40, no. 5, pp. 885-890, May 1995.
- [10] W. E. Dixon, E. Zergeroglu, D. M. Dawson, and M. W. Hannan, "Global adaptive partial state feedback tracking control of rigid-link flexible-joint robots," *Robotica*, vol. 18, no. 3, pp. 325-336, 2000.
- [11] M. S. Kim and J. S. Lee, "Adaptive tracking control of flexible-joint manipulators without overparameterization," *J. Robot. Syst.*, vol. 12, no. 7, pp. 369-379, 2004.
- [12] R. Gourdeau and H. M. Schwartz, "Adaptive control of robotic manipulators: experimental results," in *Proc. IEEE Conf. Robot. Autom.*, Sacramento, CA, Apr. 1991, pp. 8-15.
- [13] V. Lertpiriyasuwat and M. C. Berg, "Adaptive real-time estimation of end-effector position and orientation using precise measurements of end-effector position," *IEEE/ASME Trans. Mechatronics*, vol. 11, no. 3, pp. 304-319, Jun. 2006.
- [14] A. Timcenko and N. Kircanski, "Control of robots with elastic joints: Deterministic observer and Kalman filter approach," in *Proc. IEEE Conf. Robot. Autom.*, Nice, France, May 1992, pp. 722-727.
- [15] M. G. Hollars and R. H. Cannon Jr., "Experimental implementation of a nonlinear estimator in the control of flexible joint manipulators," In *Automatic Control in Aerospace: Selected Papers from the 1989 IFAC Symposium*, ed. T. Nishimura, 133-140. Oxford, UK: Pergamon, 1990.
- [16] T. Kobayashi, D. L. Simon and J. S. Litt, "Applications of a constant gain extended Kalman filter for in-flight estimation of aircraft engine performance parameters," Technical Report TM-2005-213865, NASA, September 2005.
- [17] C. A. Lightcap and S. A. Banks, "An extended Kalman filter for real-time estimation and control of a rigid-link flexible-joint manipulator," *IEEE Trans. Control Syst. Technol.*, vol. 18, no. 1, pp. 91-103, 2010.
- [18] T. Hidaka, T. Ishida, Y. Zhang, M. Sasahara and Y. Tanioka, "Vibration of a strain-wave gearing in an industrial robot," in *Proc. ASME Int. Power Trans. and Gearing Conf.*, 1990, pp.789-794.
- [19] M. W. Spong, "Modeling and Control of Elastic Joint Robots," *J. Dyn. Syst., Meas., Contr.*, vol. 109, no. 4, pp. 310-319, 1987.
- [20] S. Ulrich and J. Z. Sasiadek, "Modeling and direct adaptive control of a flexible joint manipulator," *J. Guid., Contr., Dynam.*, submitted.
- [21] N. M. Kircanski and A. A. Goldenberg, "An experimental study of nonlinear stiffness, hysteresis, and friction effects in robot joints with harmonic drives and torque sensors," *The Int. J. of Robot. Res.*, vol. 16, no. 2, 1997, pp. 214-239.
- [22] F. L. Lewis, *Optimal estimation with an introduction to stochastic control theory*, Wiley, New York, 1986, Chap. 2.4, pp. 88-94.
- [23] S. Ulrich and J. Z. Sasiadek, "Direct model reference adaptive control of a flexible joint robot," in *Proc. AIAA Guidance, Navigation and Control Conf.*, Toronto, Canada, Aug. 2010.

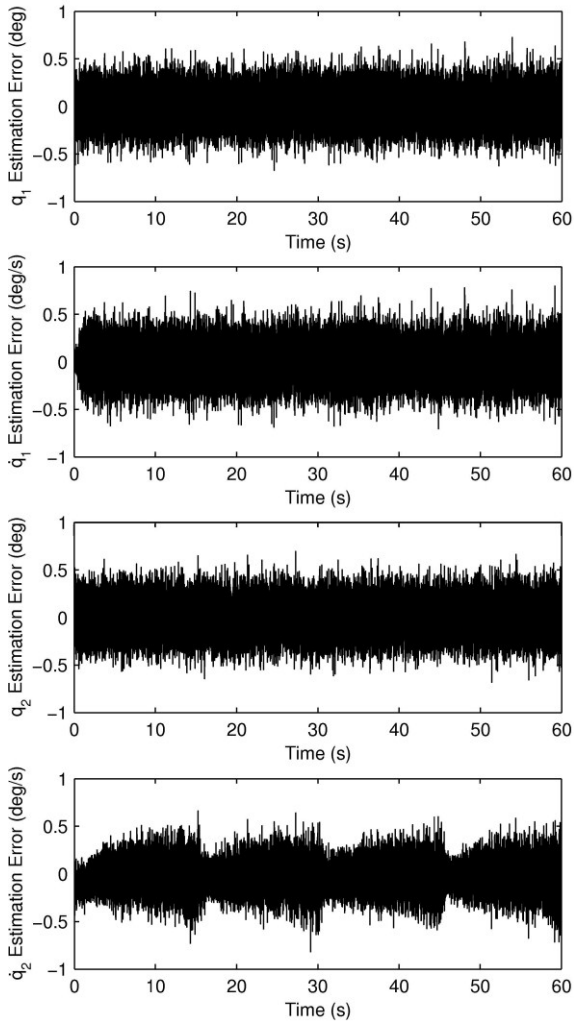


Fig. 1. Linear joint-based EKF estimation results.

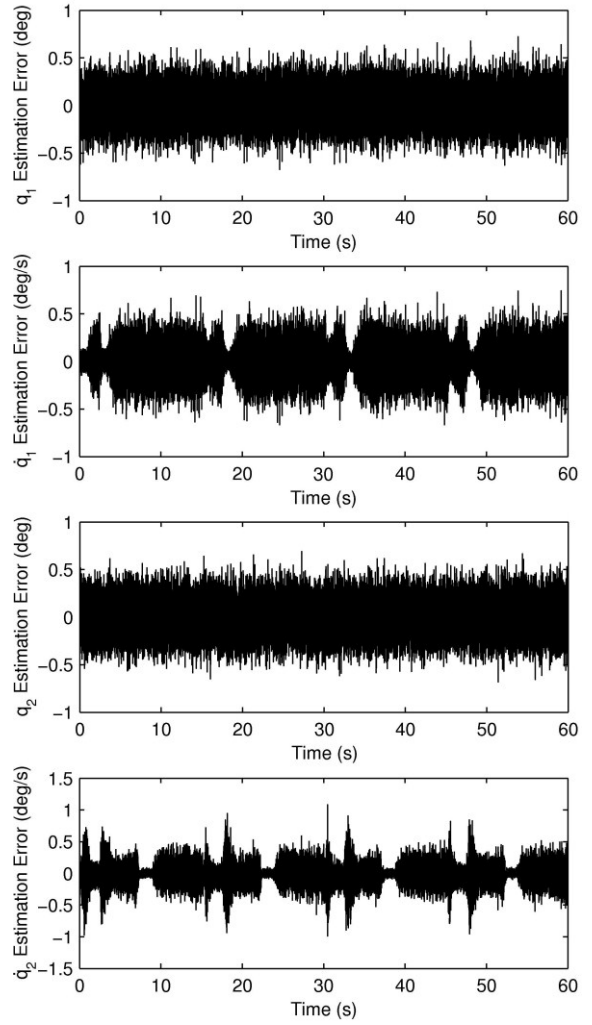


Fig. 2. Nonlinear joint-based EKF estimation results.

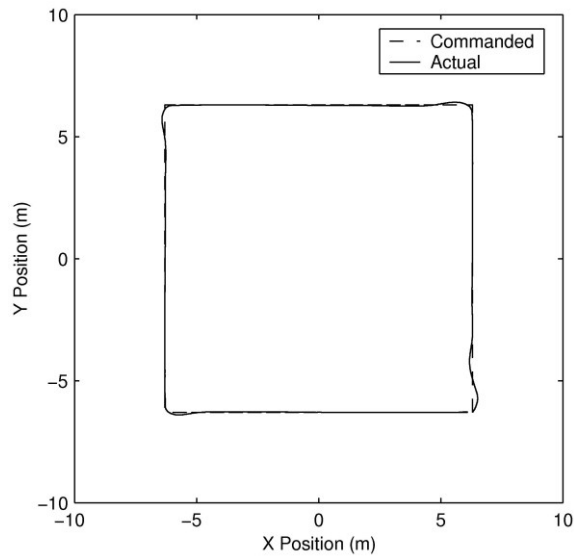


Fig. 3. Linear joint-based EKF-adaptive controller tracking results.

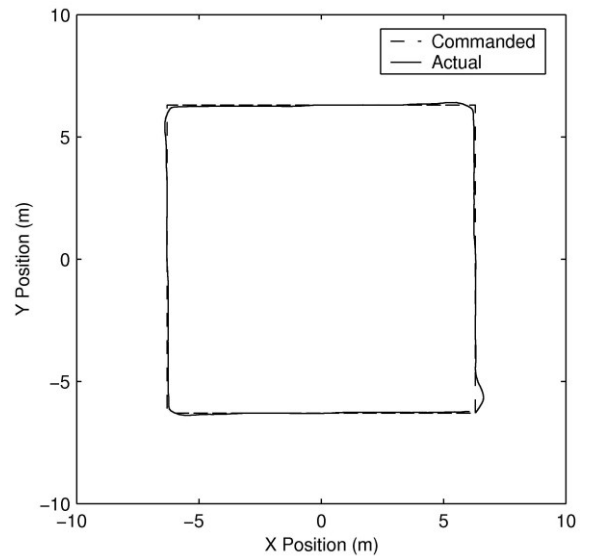


Fig. 4. Nonlinear joint-based EKF-adaptive controller tracking results.